J|A|C|S
ARTICLES
Published on Web 03/18/2003

2-Aminopyrimidine Directed Self-Assembly of Zinc Porphyrins Containing Bulky 3,5-Di-*tert*-butylphenyl Groups

Teodor Silviu Balaban,*[,†] Richard Goddard,[‡] Myriam Linke-Schaetzel,[†] and Jean-Marie Lehn*[,†,§]

Contribution from the Forschungszentrum Karlsruhe, Institute for Nanotechnology, Postfach 3640, D-76021 Karlsruhe, Germany, Max-Planck-Institut für Kohlenforschung, Kaiser-Wilhelm-Platz 1, D-45470 Mülheim an der Ruhr, Germany, and ISIS, Université Louis Pasteur, 8, rue Gaspard Monge, F-67000 Strasbourg, France

Received December 2, 2002; E-mail: silviu.balaban@int.fzk.de; lehn@int.fzk.de

Abstract: The 2-aminopyrimidin-5-yl ligand is revealed to be a promising candidate for the construction of supramolecular porphyrin arrays with broad absorption bands for efficient light-harvesting. 10-Mono- and 10,20-di(2-aminopyrimidin-5-yl) derivatives of 5,15-bis(3,5-di-*tert*-butylphenyl)porphyrin have been synthesized in high yield. Their Zn(II) salts show variable concentration and temperature-dependent UV/vis spectra in solution, consistent with supramolecular aggregation. Whereas the FAB mass spectra of the monosubsituted derivative in toluene suggest the formation of a tetramer at high concentrations and low temperatures (estimated association free enthalpy $\Delta H = 220 \pm 10$ kJ/mol), the larger splitting of the Sorret band (ca. 40 nm) in the variable temperature UV/vis spectra of the disubstituted bis(3,5-di-*tert*-butylphenyl)porphyrin is indicative of yet higher aggregates involving both 2-aminopyrimidin-5-yl groups. The tetrameric nature of the monosubsituted derivative is confirmed by X-ray analysis, which reveals that two of the 2-aminopyrimidin-5-yl groups are encapsulated by the aggregate and consequently are prevented from undergoing hydrogen bonding. NMR studies show there is no exhange of the 2-aminopyrimidin-5-yl groups, so the tetramer is rigid, which is confirmed by molecular modeling calculations. The tetramer formation is governed by $\pi-\pi$ interactions, metal coordination, and hydrogen bonding. The di(2-aminopyrimidin-5-yl) derivative forms strongly scattering solutions, which upon standing form green flocculate precipitates, reminiscent of shaken suspensions of bacteriochlorophyll *c*.

Mimicking the self-assembly ability of bacteriochlorophyll *c*,[1,2] the main pigment of chlorosomes (green sacs), the light-harvesting organelles of green photosynthetic bacteria, promises to give access to artificial and robust devices for photochemical energy conversion.[3,4] Studies on the natural system indicate that magnesium ligation in conjunction with hydrogen bonds and $\pi-\pi$ interactions are important in the self-assembling process, but as yet there is no direct structural evidence of how this occurs. A few semisynthetic mimics, as free base or with zinc instead of magnesium in the tetrapyrrolic macrocycle, have been crystallized either as monomers[5] or as dimeric assemblies.[6] Crystal structures of supramolecular assemblies of porphyrins have been recently described,[1,7] and a number of supramolecular assemblies involving porphyrins have been characterized by other techniques.[8−10]

† Institute for Nanotechnology.
‡ Max-Planck-Institut für Kohlenforschung.
§ ISIS, Université Louis Pasteur. Alternate e-mail: lehn@chimie.u-strasbg.fr.

(1) Balaban, T. S.; Eichhöfer, A.; Lehn, J.-M. *Eur. J. Org. Chem.* **2000**, 4047−4057.
(2) (a) Balaban, T. S.; Holzwarth, A. R.; Schaffner, K.; Boender, G.-J.; de Groot, H. J. M. *Biochemistry* **1995**, *34*, 15259−15266. (b) Jesorka, A.; Balaban, T. S.; Holzwarth, A. R.; Schaffner, K. *Angew. Chem., Int. Ed. Engl.* **1996**, *35*, 2861−2863. (c) Balaban, T. S.; Tamiaki, H.; Holzwarth, A. R.; Schaffner, K. *J. Phys. Chem.* **1997**, *101*, 3424−3431. (d) Balaban, T. S.; Leitich, J.; Holzwarth, A. R.; Schaffner, K. *J. Phys. Chem. B* **2000**, *104*, 1362−1372.
(3) For recent reviews on solar energy conversion, see: (a) Grätzel, M. *Nature* **2001**, *414*, 338−344. (b) Grätzel, M.; Moser, J.-E. In *Electron Transfer in Chemistry*, Vol. 5; Balzani, V., Ed.; Wiley-VCH: Weinheim, Germany, 2001; pp 589−644.
(4) (a) Bach, U.; Lupo, D.; Comte, P.; Moser, J. E.; Weissörtel, F.; Salbeck, J.; Spreitzer, H.; Grätzel, M. *Nature* **1998**, *395*, 583−585. (b) Brabec, C. J.; Shaheen, S. E.; Fromherz, T.; Padinger, F.; Hummelen, J. C.; Dhanabalan, A.; Janssen, R. A. J.; Sariciftci, N. S. *Synth. Met.* **2001**, *121*, 1517−1520.
(5) (a) Barkigia, K. M.; Fajer, J.; Smith, K. M.; Williams, G. J. B. *J. Am. Chem. Soc.* **1981**, *103*, 5890−5893. (b) Smith, K. M.; Goff, D. A.; Fajer, J.; Barkigia, K. M. *J. Am. Chem. Soc.* **1982**, *104*, 3747−3749.
(6) (a) Stibrany, R. T.; Vasudevan, J.; Knapp, S.; Potenza, J. A.; Emge, T. J.; Schugar, H. J. *J. Am. Chem. Soc.* **1996**, *118*, 3980−3981. (b) Vasudevan, J.; Stibrany, R. T.; Bumby, J.; Knapp, S.; Potenza, J. A.; Emge, T. J.; Schugar, H. J. *J. Am. Chem. Soc.* **1996**, *118*, 11676−11677. (c) Barkigia, K. M.; Melamed, D.; Sweet, R. M.; Smith, K. M.; Fajer, J. *Spectrochim. Acta Part A* **1997**, *53A*, 463−469.
(7) (a) Kumar, R. K.; Balasubramanian, S.; Goldberg, I. *Chem. Commun.* **1998**, 1435−1436. (b) Sharma, C. V. K.; Broker, G. A.; Huddleston, J. G.; Baldwin, J. W.; Metzger, R. M.; Rogers, R. D. *J. Am. Chem. Soc.* **1999**, *121*, 1137−1144. (c) Fan, J.; Whiteford, J. A.; Olenyuk, B.; Levin, M. D.; Stang, P. J.; Fleischer, E. B. *J. Am. Chem. Soc.* **1999**, *121*, 2741−2752. (d) Burrell, A. K.; Jones, B. M.; Hall, S. B.; Officer, D. L.; Reid, D. C. W.; Wild, K. Y.; *J. Inclusion Phenom. Macrocycl. Chem.* **1999**, *35*, 185−190. (e) Iengo, E.; Milani, B.; Zangrando, E.; Geremia, S.; Alessio, E. *Angew. Chem., Int. Ed.* **2000**, *39*, 1096−1099. (f) Kondo, M.; Kimura, Y.; Wada, K.; Mizutani, T.; Ito, Y.; Kitagawa, S. *Chem. Lett.* **2000**, 818−819. (g) Fujita, N.; Biradha, K.; Fujita, M.; Sakamoto, S.; Yamaguchi, K. *Angew. Chem., Int. Ed.* **2001**, *40*, 1718−1721. (h) Shi, X.; Barkigia, K. M.; Fajer, J.; Drain, C. M. *J. Org. Chem.* **2001**, *66*, 6513−6522. (i) Redman, J. E.; Feeder, N.; Teat, S. J.; Sanders, J. K. M. *Inorg. Chem.* **2001**, *40*, 2486-2499. (j) Bond, A. D.; Feeder, N.; Teat, S. J.; Clyde-Watson, Z.; Bampos, N.; Sanders, J. K. M. *Acta Crystallogr.* **2001**, *E57*, m454−m456.
(8) (a) Drain, C. M.; Fischer, R.; Nolen, E. G.; Lehn, J.-M. *J. Chem. Soc., Chem. Commun.* **1993**, 243−245. (b) Drain, C. M.; Lehn, J.-M. *J. Chem. Soc., Chem. Commun.* **1994**, 2313−2315. (c) Drain, C. M.; Russel, K. C.; Lehn, J.-M. *Chem. Commun.* **1996**, 337−338.

The current approach for devising 2−100 nanometer functional devices for photonic applications involves linking chromophoric (in our case porphyrinic) building blocks together using covalent bonds.[11,12] Such covalent multichromophoric systems have been shown to fully function as antennas and energetic traps as well as artificial reaction centers.[13] They require complicated and multistep syntheses, which limit their availability and applicability. An alternative approach is to construct tailored tectons that carry the chromophoric functionality and equip these by high-yielding synthetic steps with groups capable of inducing self-assembly. In the ideal case, the architecture and function of the final self-assembled structure is encoded in the monomeric chromophore and its substituents.[14]

The 2-aminopyrimidin-5-yl group has already been employed for engineering supramolecular hydrogen-bonded lattices of aromatic molecules within which other guest molecules can be entrapped, mostly by π-stacking,[15] but it has the added feature that it can function as a nitrogen ligand for metals. Here we report the use of 2-aminopyrimidine as a directing substituent and describe the self-assembling ability of the novel zinc 10,20-bis(3,5-di-*tert*-butylphenyl)-5-(2-aminopyrimidin-5-yl)porphyrin (Zn-**5**). Whereas pyridine, pyrazine, imidazole, and amines are frequent ligands encountered in crystal structures of zinc porphyrins, Zn-**5** represents for the first example in which a porphyrinic zinc atom is coordinated by a pyrimidine base.

Results and Discussion

Building blocks capable of self-assembling to form light-harvesting supermolecules need to contain a chromophore as the functional part, substituents to improve solubility, and groups responsible for inducing and directing self-assembly. For the chromophore we chose a porphyrin, included 3,5-di-*tert*-butylphenyl groups to improve solubility, and attached the 2-aminopyrimidine group for programing the self-assembly. In contrast to earlier approaches where the porphyrin macrocycle is constructed in the final synthetic steps by an appropriate method, which is usually quite low yielding, we chose to functionalize preformed porphyrins and thus have at the beginning of the reaction sequence the modest yields. This resulted not only in improved atom economy but also in easy chromatographic separations due to the fairly soluble and colored intermediates and products.

Bromination of the known 5,15-bis(3,5-di-*tert*-butylphenyl)-porphyrin (**1**)[16] in the free *meso* positions under mild conditions, followed by Stille coupling with phthalimido-protected 2-amino-5-(trimethylstannyl)pyrimidine[15c] affords both the mono- and/or the bis-coupled products **4** and **6** in good yields (Scheme 1). Deprotection with methylhydrazine is almost quantitative and leads to the free base porphyrins **5** and **7**, which can be metalated with zinc under standard conditions, leading to Zn-**5** and Zn-**7** in over 90% yields. It is worth noting that Stille coupling of the dibromoporphyrin **3** leads in addition to 11−22% (over different runs) of the monocoupled product **4**. It thus appears that the palladium catalyst also promotes some hydrogenation in addition to aryl−aryl coupling. Higher yields of the free base **5** can be obtained from Stille coupling of the monobromoporphyrin **2**. Not only does it occur with 38% conversion to the desired phthalimido protected product but also the starting porphyrin (**1**) can be cleanly separated from the reaction mixture and reused in further bromination cycles. This synthetic strategy makes use of the fact that functionalizing preformed porphyrins is a high-yield process whereas synthesizing the porphyrin macrocycle at the end of the sequence is generally low in yield. Attempts to suppress replacement of bromine by hydrogen entirely have so far been unsuccessful. Aberrant runs using excess palladium catalyst led to transfer of a triphenylphosphine group from palladium to one of the free *meso*-porphyrinic positions. This underlines the synthetical potential of *meso*-functionalization of easily accessible preformed porphyrins for preparing samples even in 10−20 g quantities.

The UV/vis absorption spectra of Zn-**5** in solution show interesting behavior. In millimolar solutions in dry toluene, the Soret band appears split; at lower concentrations a shoulder is visible at 431 nm and in very dilute solutions this shoulder is completely absent [Figure 1, Supporting Information]. Upon heating, the shoulder decreases while the Soret band sharpens and its peak shifts from 411 nm to ∼420 nm (Figure 1). At the same time the stronger Q-band is hypsochromically shifted by ∼10 nm, while the smaller Q-band almost vanishes completely (Figure 1, inset). These effects are also observed in dry chloroform [Figure 2, Supporting Information] but the available temperature range is smaller and the equilibrium is shifted less in favor of the associated species, which is formed only at higher concentrations.

The fact that sharp isosbestic points are observed (insets in Figure 1) leads us to conclude that two species are mainly

(9) (a) Sessler, J. L.; Capuano, V. L.; Burrell, A. K. *Inorg. Chim. Acta*, **1993**, *204*, 93−101. (b) Drain, C. M.; Nifiatis, F.; Vasenko, A.; Batteas, J. D. *Angew. Chem., Int. Ed.* **1998**, *2344*, 4−2347. (c) Haycock, R. A.; Yartsev, A.; Michelsen, U.; Sundstöm, V.; Hunter, C. A. *Angew. Chem., Int. Ed.* **2000**, *39*, 3616−3619. (d) Haycock, R. A.; Hunter, C. A.; James, D. A.; Michelsen, U.; Sutton, L. R. *Org. Lett.* **2000**, *2*, 2435−2438.

(10) (a) Chernook, A. V.; Rempel, U.; von Borczyskowski, C.; Shulga, A. M.; Zenkevich, E. I. *Chem. Phys. Lett.* **1996**, *254*, 229−241. (b) Kobayashi, K.; Koyanagi, M.; Endo, K.; Masuda, H.; Aoyama, Y. *Chem. Eur. J.* **1998**, *4*, 417−424. (c) Willert, A.; Bachilo, S.; Rempel, U.; Shulga, A.; Zenkevich, E.; von Borczyskowski, C. *J. Photochem. Photobiol. A Chem.* **1999**, *126*, 99−109. (d) Ruhlmann, L.; Schulz, A.; Giraudeau, A.; Messerschmidt, C.; Fuhrhop, J.-H. *J. Am. Chem. Soc.* **1999**, *121*, 6664−6667. (e) Ogawa, K.; Kobuke, Y. *Angew. Chem., Int. Ed.* **2000**, *39*, 4070−4073. (f) Nagata, N.; Kugimiya, N. S.; Kobuke, Y. *Chem. Commun.* **2001**, 689−690. (g) Ogawa, K.; Zhang, T.; Yosihara, K.; Kobuke, Y. *J. Am. Chem. Soc.* **2002**, *124*, 22−23.

(11) For reviews, see: (a) Vicente, M. G. H.; Jaquinod, L.; Smith, K. M. *Chem. Commun.* **1999**, 1771−1782. (b) Burrell, A. K.; Officer, D. L.; Plieger, P. G.; Reid, D. C. W. *Chem. Rev.* **2001**, *101*, 2751−2796.

(12) (a) Reimers, J. R.; Lü, T. X.; Crossley, M. J.; Hush, N. S. *Nanotechnology* **1996**, *7*, 424−429. (b) Taylor, P. N.; Huuskonen, J.; Rumbles, G.; Aplin, R. T.; Williams, E. Anderson, H. L. *Chem. Commun.* **1998**, 909−910. (c) Wilson, G. S.; Anderson, H. L. *Chem. Commun.* **1999**, 1539−1540. (d) Mongin, O.; Schuwey, A.; Vallot, M.-A.; Gossauer, A. *Tetrahedron Lett.* **1999**, *40*, 8347−8350. (e) Mongin, O.; Hoyler, N.; Gossauer, A. *Chem. Eur. J.* **2000**, 1193−1197. (f) Rucareanu, S.; Mongin, O.; Schuwey, A.; Hoyler, N.; Gossauer, A.; Amrein, W.; Hediger, H.-U. *J. Org. Chem.* **2001**, *66*, 4973−4988. (g) Sugiura, K.; Tanaka, H.; Matsumoto, T.; Kawai, T.; Sakata, Y. *Chem. Lett.* **1999**, 1193−1194. (h) Sugiura, K.; Fujimoto, Y.; Sakata, Y. *Chem. Commun.* **2000**, 1105−1106.

(13) (a) Holten, D.; Bocian, D. F.; Lindsey, J. S. *Acc. Chem. Res.* **2002**, *35*, 57−69. (b) Gust, D.; Moore, T. A.; Moore, A. L. *Pure Appl. Chem.* **1998**, *70*, 2189−2200.

(14) Lehn, J.-M. *Supramolecular Chemistry. Concepts and Perspectives*, VCH: Weinheim, 1995.

(15) (a) Krische, M. J.; Lehn, J.-M.; Kyritsakas, N.; Fischer, J. *Helv. Chim. Acta* **1998**, *81* 1909−1920. (b) Krische, M. J.; Lehn, J.-M.; Kyritsakas, N.; Fischer, J.; Wegelius, E. K.; Nissinen, M. J.; Rissanen, K. *Helv. Chim. Acta* **1998**, *81* 1921−1930. (c) Krische, M. J.; Lehn, J.-M.; Kyritsakas, N.; Fischer, J.; Wegelius, E. K.; Rissanen, K. *Tetrahedron* **2000**, *56*, 6701−6706. (d) Balaban, T. S.; Krische, M. J.; Lehn, J.-M., unpublished results.

(16) (a) Susumu, K.; Shimidzu, T.; Tanaka, K.; Segawa, H. *Tetrahedron Lett.* **1996**, *37*, 8399−8402. (b) Bhuiyan, A. A.; Seth, J.; Yoshida, N.; Osuka, A.; Bocian, D. F. *J. Phys. Chem. B* **2000**, *104*, 10757−10764. (c) Tamiaki, H.; Nagata, Y.; Tsuduki, S. *Eur. J. Org. Chem.* **1999**, 2471−2473. (d) Tsuda, A.; Nakano, A.; Furuta, H.; Yamochi, H.; Osuka, A. *Angew. Chem., Int. Ed.* **2000**, *39*, 558−560. (e) Yoshida, N.; Aratani, N.; Osuka, A. *Chem. Commun.* **2000**, 197−198. (f) Screen, T. E. O.; Blake, I. M.; Ress, L. H.; Clegg, W.; Borwich, S. J.; Anderson, H. L. *J. Chem. Soc., Perkin Trans.*, **2002**, 320−329.

Scheme 1

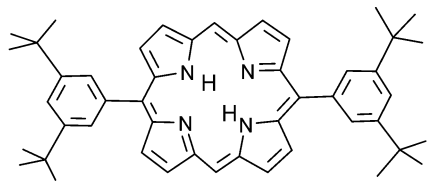

1

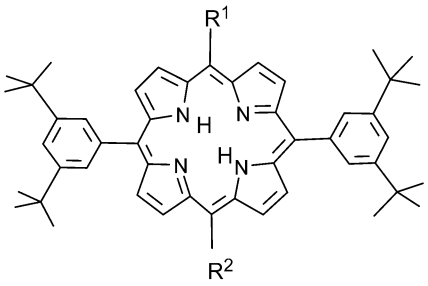

	2	3	4	5	6	7
R^1	Br	Br	PymP	Pym	PymP	Pym
R^2	H	Br	H	H	PymP	Pym

PymP :

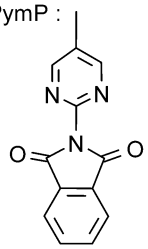

Pym :

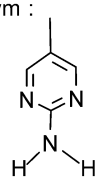

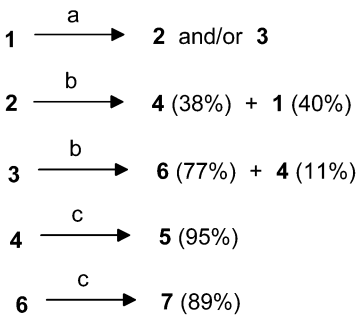

a : NBS, $CHCl_3$, pyridine, 0 °C

b :

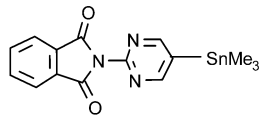

$Pd(PPh_3)_4$, PhMe, Δ

c : $MeNH\text{-}NH_2$, CH_2Cl_2

present in the anhydrous toluene or chloroform solutions. One is the monomer and the second is an associated species that exhibits an almost symmetrical (Davidov) splitting of the Soret band due to a strong excitonic interaction. Dilution or a temperature rise results in the disappearance of this self-assembled species. Careful temperature monitoring shows that upon repeated heating/cooling cycles no hysteresis behavior and no concomitant shifting of the isosbestic points occurs. This indicates that the self-assembly is fully reversible on time scales consistent with temperature equilibration. From a Van't Hoff plot using Gaussian band deconvolution and an area fit of the peaks, we estimate the association free enthalpy ΔH to be 220 $\pm$ 10 kJ/mol. If other interactions are neglected, this corresponds to the formation of at least five Zn−pyrimidine bonds, based on a zinc−pyridine ligation energy of approximately 35−40 kJ/mol and assuming that pyrimidine is a weaker ligand. A detailed modeling, as has been carried out for bacteriochlorophyll *c* where the self-assembly kinetics can be quite slow at certain concentrations,[2d] is beyond the present scope of this work. That Zn ligation is involved becomes evident from the instant disassembly achieved by titrating with a strongly zinc ligating entity such as pyridine or methanol [Figure 3, Supporting Information]. Disassembly is irreversible as long as the competing ligand has not been removed from the medium.

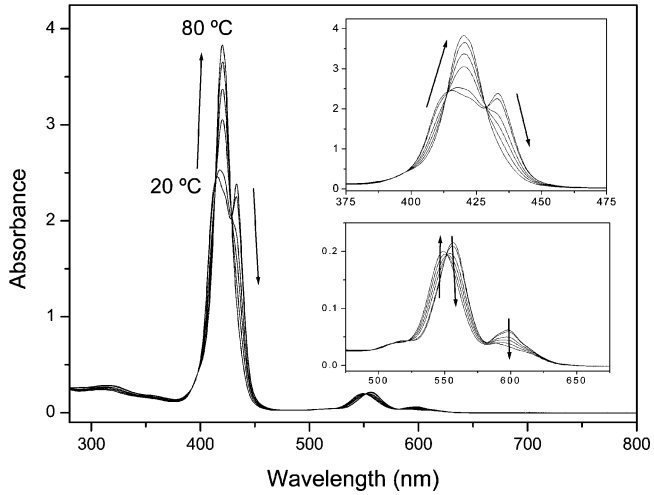

Figure 1. Variable temperature absorption spectra of Zn-**5** in toluene.

A strong indication for preferential formation of a tetrameric species came from FAB mass spectra obtained for an anhydrous toluene solution with 2-nitrophenyl octyl ether as the matrix [Figure 4, Supporting Information]. In addition to the expected monomeric peak (at m/z = 842.6 Da), much smaller dimeric and trimeric peaks are encountered. In addition, there is a peak corresponding to a tetramer at m/z = 3373.9, which is approximately 6 times more intense than that of the trimer (at m/z = 2527.6 Da), while peaks corresponding to a pentamer or hexamer are absent. It is not possible to derive stabilities of oligomeric species directly from peak intensities, but whereas dimer and trimer peaks might actually be formed by gas-phase fragmentation of the tetramers and their actual concentration in the sample toluene solution negligible, this argument does not hold for the tetramer, since higher oligomers are not observed. It is perhaps worth noting that we were unable to detect any oligomeric species other than the Zn-**5** monomer by MALDI-TOFF spectrometry using a variety of matrices. Although the ionization process is generally thought to be much milder with MALDI mass spectrometry, this observation might be due to direct photoexcitation of the porphyrin units by the laser (373 nm) resulting in a complete disassembly of the oligomers on a ns time scale. NMR spectroscopy (at 300 MHz)

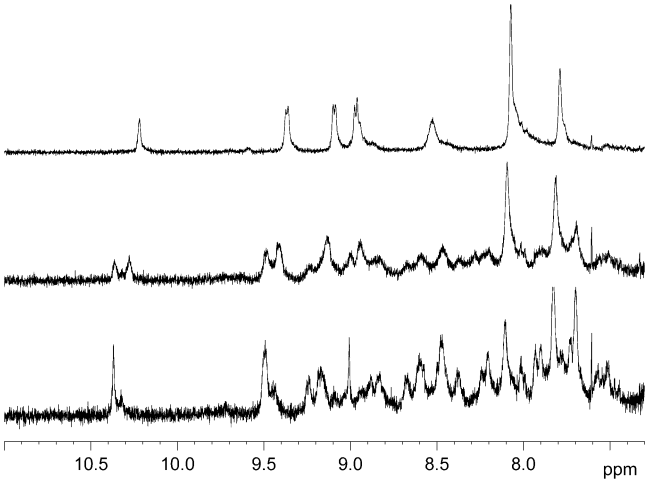

Figure 2. Low-field region of the ^{1}H NMR spectra (300 MHz) of a solution of Zn-**5** in dry $CDCl_3$ at room temperature. The lower trace is without methanol-d_4. The middle trace was recorded after addition of 10 μL of methanol-d_4, while the upper trace has been recorded after adding 30 μL of methanol-d_4. Other regions of interest are given in Figure 5 (Supporting Information).

shows quite complex spectra at room temperature, both in anhydrous toluene-d_8 or chloroform-*d*. Titration with methanol-d_4 leads to a dramatic simplification of the spectra (Figure 2).

While at low methanol concentrations both the self-assembled species and monomer are present, with excess methanol only the monomeric zinc−porphyrin−methanol complex is present. NOESY spectra of the self-assembled species indicate close contacts between aromatic protons, which resonate at high fields (two peaks at 6.0 and 6.4 ppm), and aromatic protons of the 3,5-di-*tert*-butylphenyl groups. Symmetry considerations indicate that at least two nonequivalent magnetic environments must exist for each porphyrin and each 2-aminopyrimidin-5-yl group in the self-assembled species. An additional peak at the unusually high field of −2 ppm is also present. It integrates for only one proton and can be assigned to one of the 4- or 6-pyrimidinic aromatic protons strongly shielded by porphyrinic ring current. Variable temperature experiments in $CDCl_3$ did not lead to coalescence of signals below 55 °C. However, in toluene-d_8 some of the signals start to coalesce at about 65 °C, but sharp and clean monomer signals do not appear even at higher temperatures (90 °C). Unfortunately, the monomer-associated species equilibrium is still in the slow exchange limit at the higher concentrations needed to obtain tractable NMR spectra, so the determination of reliable ΔG values is difficult. In a control experiment, we note that the NOESY spectra in the presence of methanol-d_4 showed no extra-monomeric cross-peaks.

Valuable information about the nature of the aggregate was provided by a single-crystal X-ray structure analysis.[17] Fragile, deep red crystals of Zn-**5** were grown by slow diffusion over a period of several months from a three-component system, comprising a bottom layer of the compound dissolved in chloroform separated from an upper layer of pure cyclohexane by an intermediate layer of a 1:1 mixture of chloroform/cyclohexane. The X-ray analysis reveals that the monomer units are linked head-to-tail via Zn−N coordinative bonds between one of the aromatic N atoms of the 2-aminopyrimidinyl group of one monomer and the Zn atom of a neighboring monomer

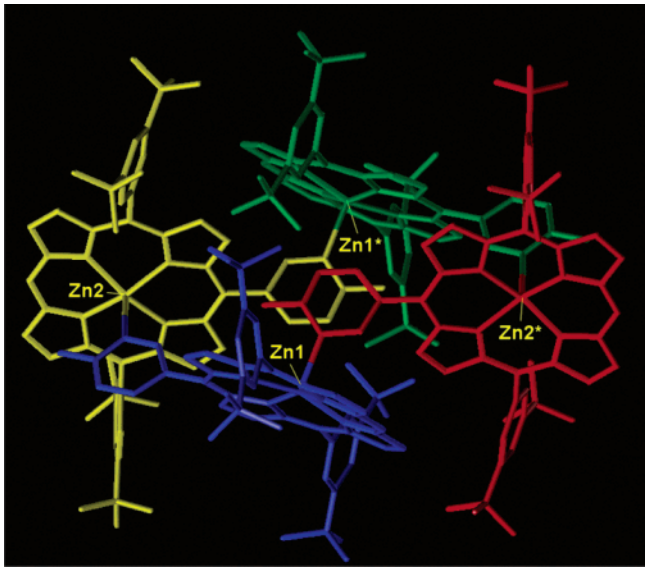

Figure 3. Structure of the Zn-**5** tetramer in the crystal.

to form a compact tetramer, in which two of the 2-aminopyrimidin-5-yl groups are located on the outside of the supramolecular species and two are buried at the center of the tetramer (Figure 3).[18] The *meta* position of the coordinating N atom with respect to the tetrapyrrole core in the 2-aminopyrimidinyl group of the monomer appears to be critical in determining the nature of the assembly, since 4-pyridyl substituents on the porphyrin ring tend to favor the formation of catemers,[19] whereas 2-pyridyl substituents lead to dimers.[6a,b]

Despite its large size, the Zn-**5** tetramer has conformationally very few degrees of freedom. Apart from the single bonds in the 3,5-di-*tert*-butylphenyl groups, there are only eight rotatable bonds in the cyclomer. Four arise from Zn−N coordination and four from pyrimidine−porphyrin bonds. Whereas the monomers adopt similar conformations, with the plane of the pyrimidinyl group lying approximately perpendicular to that of the porphyrin ring in both independent monomers (102 and 112°), the mode of the attachment of the pyrimidinyl substituent to the neighboring Zn is significantly different (Figure 3). Rotation about any of the eight rotatable bonds, however, results in strong intramolecular steric hindrance.[20] This conformational restriction provides an explanation for the adopted geometry and the inability of the independent aminopyrimidinyl ligands to ex-

(17) Crystal data for Zn-**5**·23(C_6H_{12}): red crystals from C_6H_{12}/$CHCl_3$, $(C_{52}H_{55}N_7Zn)_4$·23(C_6H_{12}), M_r = 5309.19, triclinic, space group P1 [No. 2], a = 20.108(2) Å, b = 20.637(2) Å, c = 21.073(2) Å, α = 97.473(4)°, β = 101.618(4)°, γ = 100.502(4)°, V = 8295(2) Å^3, T = 100 K, Z = 1, ρ_{calcd} = 1.06 g cm^{-3}, μ = 0.34 mm^{-1}, crystal size 0.56 × 0.73 × 0.77 mm, Siemens SMART diffractometer, Mo Kα X-radiation, 2.0 < θ < 33.09°, 90343 measured reflections, 53961 independent and 16423 with $I > 2\sigma(I)$, programs SHELXS-97 and SHELXL-97; both programs are from G. M. Sheldrick, University of Göttingen, 1997; 1693 parameters, R1 = 0.086, wR2 (all data) = 0.273, $(\sigma/\Delta)_{max}$ = 0.001, H atoms riding, C−C bonds of three cyclohexane solvate molecules were restrained to be equal (C atoms half occupancy and isotropic adp's), in one of these the chair conformation was restrained, max/min residual density 1.068/−0.699 e Å^{-3}.

(18) The four Zn atoms are coplanar and describe an approximate rhombus. Distances (Å): Zn1−Zn2 8.330(1), Zn1−Zn2* 8.558(1), Zn1−Zn1* 9.073(1). The mean planes of the two independent porphyrin macrocycles make angles of 65 and 85° to the rhombus plane, and the two central porphyrin rings (blue/green) are 8.77 Å apart.

(19) (a) Schachter, A. M. *J. Chem. Soc., Chem. Commun.* **1988**, 960−961. (b) Fleischer, E. B.; Schachter, A. M. *Inorg. Chem.* **1991**, *30*, 3763−3769. (c) Krupitsky, H.; Stein, Z.; Goldberg, I.; Strouse, C. E. *J. Inclusion Phenom. Macrocycl. Chem.* **1994**, *18*, 177−192.

(20) Program SYBYL 6.2 (Tripos Associates, Inc., St. Louis, MO); force field Tripos version 5.2, nonbonded cutoff 8 Å.

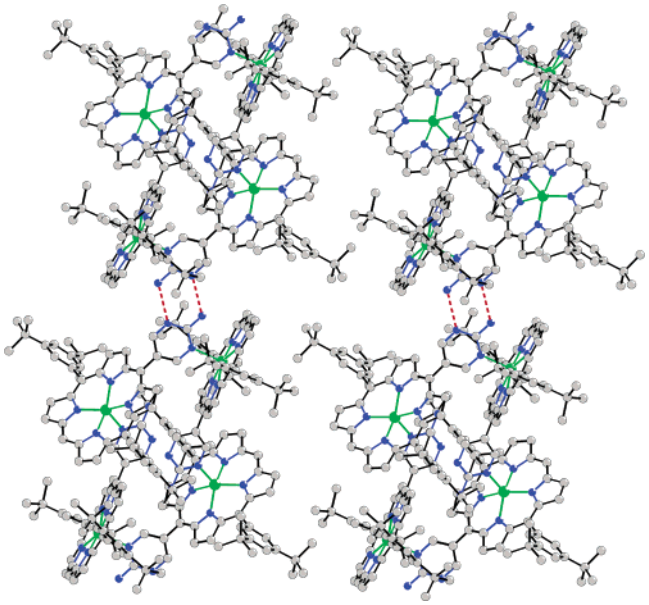

Figure 4. Four hydrogen-bonded tetramers in the crystal. Hydrogen bonds are red, nitrogen atoms are blue, zinc atoms are green, and carbon atoms are gray spheres. Cyclohexane molecules fill the voids between the tetramers and act as binder. These have been omitted for clarity.

hange. The monomers are thus not only strongly linked to one another by Zn−N coordinative bonds but their surfaces are also close-packed. As a result, there is no solvent molecule occluded in the tetramer, and despite their propensity to form double N−H···N hydrogen bonds,[15] two of the polar aminopyrimidine ligands at the center of the tetramer are not involved in further hydrogen bonding.[21]

The 2-aminopyrimidinyl group is engaged in three different supramolecular interactions within the crystal. First, it is coordinated to the Zn atom via one of the aromatic N atoms (Zn−N 2.211(4) Å).[22] Second, the two 2-aminopyrimidinyl groups in the interior of the tetramer form an off-set π-stacked arrangement with an interplanar distance of 3.32(2) Å, which is comparable to that in graphite (3.35 Å). Finally, the two remaining 2-aminopyrimidinyl groups are involved in double N−H···N hydrogen bonds to neighboring tetramer units, forming a catemer of tetramers (Figure 4). The N−H···N distance at 2.992(6) Å is shorter than that observed in crystalline 2-aminopyrimidine (3.06 Å)[23] or 2-amino-5-nitropyrimidine (3.05 Å)[24] and indicates that there is some relation between the zinc ligation of the 1-N atom and the basicity of the 3-N atom in the pyrimidine ring. Semiempirical calculations (PM3) support this.[25] It is important to note that the inter-tetramer hydrogen bonding is only expected to become effective when the medium becomes nonpolar, such as when cyclohexane displaces the better solvating chloroform.

Apart from the double N−H···N hydrogen bonds involving the external 2-aminopyrimidinyl groups, there are no other direct interactions between the tetramers in the crystal. In dry chloroform solution, the hydrogen bonding ability of the

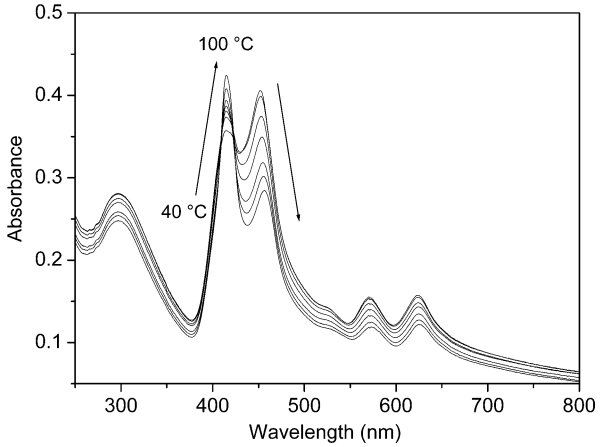

Figure 5. Heating of a suspension of self-assembled Zn-**7** in dry *n*-heptane. The sample was prepared by diluting a chloroform solution of Zn-**7** with a 50-fold excess of *n*-heptane. The nonzero absorption at 800 nm is due to light scattering. Note that complete disassembly does not occur even at 100 °C.

2-aminopyrimidin-5-yl groups is too weak to lead to any preorganization of the tetramers. This is supported by ^{1}H NMR studies of soluble 9,10-bis(2-aminopyrimidin-5-yl)anthracene derivatives.[15d] Although the crystals were grown from chloroform/cyclohexane, they contain no chloroform and each tetramer is surrounded by 26 cyclohexane sites.[26] The crystal can thus be described as a solid solution, containing approximately 60% cyclohexane by weight, which is apparently held together by relatively strong cohesive forces.[27] The large amount of solvent in the crystal lattice explains the extreme sensitivity of the crystals to the atmosphere, which causes the crystals to disintegrate through loss of solute. Although porphyrin sponges and porphyrin zeolithes have been described before,[28] this structure differs from those previously described in the sense that the solvent molecules are not clathrated inside voids but rather serve as a cement for the hydrogen-bonded catemers of tetramers. Construction of discrete assemblies of chromophores with tailored photophysical properties, such as broad and red-shifted absorption bands, suggest the possibility of using these as energetic traps to capture light from a supramolecular antenna.

Quite a different architecture of self-assembled Zn-**7** occurs. Both *meso*-linked 2-aminopyrimidine groups are involved in ligating zinc atoms of neighboring molecules, as can be inferred from the greater splitting of the Soret band (almost 40 nm) and the temperature behavior in different solvents (Figure 5). Much larger nanostructures must be formed since the solutions scatter light strongly and eventually deposit green fluffs. This behavior is similar to that encountered for bacteriochlorophyll *c*, where shearing forces are sufficient to disrupt the assemblies so that suspensions of it become homogeneous upon shaking or short sonication.[2d] In contrast to self-assembled Zn-**5**, where the process was reversible at higher temperatures in toluene or

(21) Hydrogen bonding is presumably prevented by encapsulation of the aminopyrimidinyl groups by the self-association of [Zn-**5**]$_4$.
(22) Although coordination of the amine function to the metal is also conceivable, there is no evidence that this ever occurs in the case of 2-aminopyrimidine.
(23) Furberg, S.; Grogaard, G.; Smedsnid, B. *Acta Chem. Scand. Ser. B* **1979**, *33*, 715−724.
(24) Aakeroy, C. B.; Nieuwenhuyzen, M.; Price, S. L. *J. Am. Chem. Soc.* **1998**, *120*, 8986−8993.
(25) While the noncoordinating pyrimidinic nitrogens have negative partial charges (−0.17), ligation of a porphyrinic zinc atom leads to a partial positive charge (+0.11) which enhances the polarization of the neighbouring N−H bonds leading to tighter inter-tetrameric hydrogen bonding.
(26) Six of the sites are only half occupied in the crystal, resulting in a molecular formula containing 23 cyclohexane molecules.
(27) Dunitz, J. D.; Gavezzotti, A. *Acc. Chem. Res.* **1999**, *32*, 677−684.
(28) (a) Byrn, M. P.; Curtis, C. J.; Khan, S. I.; Sawin, P. A.; Tsurumi, R.; Strouse, C. E. *J. Am. Chem. Soc.* **1990**, *112*, 1865−1874. (b) Kumar, K. R.; Goldberg, I. *Chem. Commun.* **1998**, 1435−1436. (c) Diskin-Posner, Y.; Goldberg, I. *Chem. Commun.* **1999**, 1961−1962. (d) Diskin-Posner, Y.; Dahal, S.; Goldberg, S, I. *Angew. Chem., Int. Ed.* **2000**, *39*, 1288−1292.

chloroform, in the case of Zn-**7** the equilibrium is shifted strongly on the side of the self-assembled species. Only in the presence of zinc-competing ligands, such as methanol, does irreversible deassociation occur [Figure 6, Supporting Information]. Attempts to characterize assemblies of Zn-**7** by FAB-MS met with failure due to the their higher oligomeric nature compared with that of Zn-**5**. However, size exclusion chromatography by gel permeation using nonpolar eluents such as various toluene−*n*-hexane mixtures shows numerous broad oligomeric peaks which are eluted before a large monomeric peak as inferred from its unperturbed Soret absorption band.

Conclusion

The introduction of one 2-aminopyrimidine group into a *meso* position of a porphyrin results in a molecule whose Zn complex is capable of self-associating to form a rigid tetramer, with optical properties different from those of the monomer. Formation of the tetramer is reversible and is affected by temperature rise and coordinating solvents. In addition to metal ligation, the 2-aminopyrimidine group is involved in different supramolecular interactions depending on its location in the tetramer. In the center of the tetramer it undergoes $\pi-\pi$ interactions, whereas on the surface it is capable of forming N−H···N hydrogen bonding to neighboring tetramers in nonpolar solvents. A different self-assembly pattern occurs when two 2-aminopyrimidine groups are present in opposite *meso*-positions of the porphyrin ring. Clearly, the geometry of the final self-associated species is directed by the interactional features contained within the structure of the monomeric species. Further investigations into the nature of the self-assembly of the bis(2-aminopyrimidinyl)-porphyrin **7** and its zinc complex Zn-**7** are currently in progress. The photophysical properties (time-resolved fluorescence and transient absorption) of films cast either from Zn-**5** or Zn-**7** are of interest with a view to designing artificial antenna systems by using self-assembly, and these will be reported in due course.

Experimental Section

General Remarks. Solvents were dried and freshly distilled before use as follows: dichloromethane over calcium hydride; toluene over sodium metal; chloroform-*d* over phosphorus pentoxide. NMR spectra were recorded at 300 MHz (^{1}H) with a Bruker DPX 300 Avance spectrometer. Chemical shifts are given in ppm relative to the signal of $CHCl_3$, which was taken as $\delta = 7.26$ (for ^{1}H) and 77.00 (for ^{13}C). UV/vis spectra were measured with a Varian Cary 500 equipped with a Peltier variable temperature unit. Temperature control was better than 0.1° as measured in a separate reference cuvette. Gel-permeation HPLC was performed on a Varian ProStar machine equipped with a preparative (250 × 21 mm) Nucleogel GPC 500-10 column from Macherey-Nagel. FT-IR spectra were obtained on a Perkin-Elmer Spectrum GX spectrometer as KBr pellets. MALDI-TOFF mass spectra were obtained on a Voyager Instrument from Applied Biosystems either with anhydrous glycerol or HABA [2′-(4-hydroxyphenylazo)benzoic acid] matrices. FAB mass spectra were obtained with a Micromass Autospec instrument using 2-nitrophenyl octyl ether as a nondissociating matrix. HR-FAB-MS results were recorded with 3-nitrobenzyl alcohol as the matrix on a Finnigan MAT 90 machine. The crystal diffraction data were collected with a Siemens SMART diffractometer. Elemental analyses were performed with a CE Flash 400 Instrument. Retention factors are given for silica gel TLC plates (Macherey-Nagel), which were eluted with dichloromethane stabilized with 0.2% ethanol unless otherwise stated. Column chromatography was performed with Merck silica gel 40−63 μm.

5-Bromo-10,20-bis(3,5-di-*tert*-butylphenyl)-21*H*,23*H*-porphine (2). Porphyrin **1** (250 mg, 0.36 mmol) was dissolved in 90 mL of dichloromethane and 0.5 mL of pyridine added. NBS (65 mg, 0.36 mmol) was added in portions and the mixture stirred at room temperature for 4 h after which it was quenched with 10 mL of acetone. After stirring for 15 min, the solvents were evaporated and the residue was chromatographed on silica gel eluted with a mixture of dichloromethane−*n*-hexane (1:9 v/v). The product had $R_F = 0.8$ or 0.5 (TLC eluted with dichloromethane−*n*-hexane (6:4 v/v) or (3:7 v/v), respectively. ^{1}H NMR ($CDCl_3$), $\delta = 10.20$ (s, 1H, 15-H), 9.78 (d, ^3J(H,H) = 4.8 Hz, 2H, 3,7-H), 9.32 (d, ^3J(H,H) = 4.8 Hz, 2H, 13,17-H), 9.03 (two d, ^3J(H,H) = 4.5 Hz, 4H, 2,8,12,18-H), 8.11 (d, ^4J(H,H) = 2.0 Hz, 4H, 2″,6″-H), 7.86 (t, ^4J(H,H) = 1.8 Hz, 4H, 4″-H), 1.58 (s, 36H, $C(CH_3)_3$), −2.90 (s, 2H, 21,23-H). ^{13}C NMR ($CDCl_3$), δ = 31.7 ($C(CH_3)_3$), 35.0 ($C(CH_3)_3$), 103.4 (C-5), 105.4 (C-15), 121.3 (4"-C), 121.7 (10,20-C), 130.0 (2″,6″-C), 131.0 (broad, 13,17-C), 131.5 (broad 2,8- and 12,18-C), 132.3 (broad, 3,7-C), 140.4 (1"-C), 149.0 (3″,5″-C). UV ($CHCl_3$) λ_{max}, log(ϵ_{max}): 418 (4.51), 514 (3.15), 549 (2.76), 590 (2.64), 646 (2.54). IR (KBr) 630 w, 690 mw, 715 m, 731 m, 762 w, 791 s, 807 mw 846 mw, 881mw, 917 m, 964 m, 971 m, 1049 w, 1245 m, 1362 m, 1475 w, 1591 ms, 2858 m, 2899 m, 2963 s, 3311 mw. MALDI-TOFF-MS (glycerol matrix): $m/z = 765.43$ (100) [M + H$^+$]. HR-FAB-MS: $m/z = 766.3623$; calcd for $C_{48}H_{55}BrN_4 = 766.3610$ (for the main isotopomer).

5,15-Dibromo-10,20-bis(3,5-di-*tert*-butylphenyl)-21*H*,23*H*-porphine (3). Porphyrin **1** (832 mg, 1.21 mmol) was dissolved in 300 mL of chloroform and 1.25 mL of pyridine was added; then the reaction mixture was cooled to 0 °C before addition of NBS (431 mg, 2.42 mmol). After stirring for 10 min, the reaction was quenched by addition of 20 mL of acetone. The solvents were then removed in a vacuum, and the residue was washed with methanol several times followed by washing with *n*-hexane. This produced in 75% yield (760 mg) a pure sample (by NMR) which was suitable for further transformations after drying (10^{-1} Torr). An analytical sample was recrystallized from a hot hexane−chloroform (1:1) solution. ^{1}H NMR ($CDCl_3$), $\delta = 9.62$ (d, ^3J(H,H) = 4.8 Hz, 4H, 2,8,12,18-H), 8.88 (d, ^3J(H,H) = 4.5 Hz, 4H, 3,7,13,17-H), 8.02 (d, ^4J(H,H) = 1.8 Hz, 4H, 2″,6″-H), 7.85 (t, ^4J(H,H) = 1.8 Hz, 4H, 4″-H), 1.59 (s, 36H, $C(CH_3)_3$), −2.70 (s, 2H, 21,23-H). Solubility in $CDCl_3$ or DMSO-d_6 was too low to obtain meaningful ^{13}C NMR spectra (only the *tert*-butyl signals at 31.7 and 35.1 ppm and *tert*-butylphenyl proton bearing aromatic carbons at 122.8 and 129.9 ppm were visible in an overnight spectrum). UV ($CHCl_3$) λ_{max}, log(ϵ_{max}): 424 (4.51), 523 (3.17), 559 (3.04), 603 (2.65), 661 (2.80). IR (KBr): 629 w, 711 m, 729 mw, 793 s, 808 w, 881 mw, 917 mw, 972 s, 1243 m, 1362 m, 1468 mw, 1592 m, 2865 mw, 2899 mw, 2963 s, 3318mw. MALDI-TOFF-MS (glycerol matrix): $m/z = 844.38$ (100) [M$^+$]. HR-FAB-MS: $m/z = 843.2620$; calcd for $C_{48}H_{53}N_4Br_2 = 843.2637$ (for the main isotopomer).

5-(2-Phthalimidopyrimidin-5-yl)-10,20-bis(3,5-di-*tert*-butylphenyl)-21*H*,23*H*-porphine (4). Argon was bubbled for 5 min through a suspension of the monobromoporphyrine **2** (20 mg, 0.026 mmol) and of 2-phthalimido-5-(trimethylstannyl)pyrimidine[15c] (12 mg, 0.031 mmol) in 4 mL of dry toluene. The catalyst tetrakis(triphenylphosphine)-palladium (1.5 mg, 0.05 mol %) was then added, and the mixture was degassed with argon for a further minute and then stoppered and heated on an oil bath at 105 °C for 100 h. After cooling to room temperature, 1 g of silica gel was added and the solvent was removed in a vacuum. Column chromatography on silica gel eluting with a mixture of dichloromethane−*n*-hexane (1:1, v/v) produced a first fraction of porphyrin **1** (3.5 mg, 17% yield), a second fraction of unreacted **2** (8.5 mg, 38% yield), and finally the coupled product **4** (9.0 mg, 38%). ^{1}H NMR ($CDCl_3$), $\delta = 10.31$ (s, 1H, 15-H), 9.73 (s, 2H, 4′,6′-pyrymidinic-H), 9.39 (d, ^3J(H,H) = 4.5 Hz, 2H, 13,17−H), 9.11 (d, ^3J(H,H) = 4.8 Hz, 2H, 12,18−H), 9.09 (d, ^3J(H,H) = 4.8 Hz, 4H, 2,8−H), 8.90 (d, ^3J(H,H) = 4.8 Hz, 2H, 3,7−H), 8.15 (dd, ^3J(H,H) = 5.4 Hz, ^4J(H,H) = 3.0 Hz, 2H, phthalimido-H), 8.13 (d, ^4J(H,H) = 1.8 Hz, 4H, 2″,6″-H), 7.93 (dd, ^3J(H,H) = 5.7 Hz, ^4J(H,H) = 3.0 Hz, 2H, phthalimido-H), 7.85 (t, ^4J(H,H) = 1.8 Hz, 4H, 4"-H), 1.57 (s, 36H, $C(CH_3)_3$), −2.95

(s, 2H, 21,23-H). ^{13}C NMR ($CDCl_3$), δ = 31.7 ($C(CH_3)_3$), 35.1 ($C(CH_3)_3$), 106.2 (15-C), 109.9 (5-C), 121.3, 121.9 (4″-C), 124.4 (phthalimido-C), 130.0, 130.2 (2″,6″-C), 131.5 (broad, 3,7-C), 133.2 (broad, 13,17-C), ~134.0 (broad, 2,8- and 3,7-C), 134.9 (phthalimido-C), 135.8, 140.4, 149.1, 152.7 (4′,6′-C), 161.3, 166.0 (C=O). Assignments are based on H−C and H−H correlated spectra as well as a NOESY experiment. UV ($CHCl_3$) λ_{max}, log(ϵ_{max}): 418 (3.57), 447 (3.30), 513 (3.21), 548 (2.80), 586 (2.77), 641 (2.64). IR ($CHCl_3$): 932 w, 1602 s, 1728, m, 2856, m, 2928 s, 2961 m. MALDI-TOFF-MS (HABA matrix): m/z = 909.66 (100) [M^+]. HR-FAB-MS: m/z = 910.4832; calcd for $C_{60}H_{60}N_7O_2$ = 910.4808.

5-(2-Aminopyrimidin-5-yl)-10,20-bis(3,5-di-*tert*-butylphenyl)-21*H*,23*H*-porphine (5). To a solution of 27.2 mg **4** in 30 of mL dry, freshly distilled dichloromethane was added 1.5 mL of methylhydrazine, and the reaction mixture was degassed with argon for 3 min after which it was stirred for 2 h at room temperature. Silica gel (3.5 g) was added to the flask, and the solvent was removed in a vacuum (Caution: at the end of the evaporation a strongly exothermic adsorption on silica gel occurs due to the residual methylhydrazine. External cooling is recommended). Column chromatography on silica gel eluted with dichloromethane containing 5% MeOH afforded a main fraction (22.2 mg, 95% yield) with R_F = 0.62 (TLC eluted with 5% MeOH in CH_2Cl_2). ^{1}H NMR ($CDCl_3$), δ = 10.25 (s, 1H, 15-H), 9.36 (d, ^3J(H,H) = 4.5 Hz, 2H, 13,17−H), 9.11 (s, 2H, 4′,6′-pyrimidinic-H), 9.10 (d, ^3J(H,H) = 4.8 Hz, 2H, 12,18−H), 9.09 (d, ^3J(H,H) = 4.8 Hz, 4H, 2,8- or 3,7-H), 8.96 (d, ^3J(H,H) = 4.8 Hz, 2H, 3,7- or 2,8-H), 8.12 (d, ^4J(H,H) = 1.8 Hz, 4H, 2″,6″-H), 7.84 (t, ^4J(H,H) = 1.8 Hz, 4H, 4"-H), 5.47 (s, 2H, NH_2), 1.56 (s, 36H, $C(CH_3)_3$), −2.96 (s, 2H, 21,23-H). ^{13}C NMR ($CDCl_3$), δ = 31.7 ($C(CH_3)_3$), 35.1 ($C(CH_3)_3$), 105.1 (15-C), 112.7 (5-C), 121.2 (10,20-C), 121.4 (4"-C), 127.2, 130.1 (2″,6″-C), ~130 (broad 3,7- or 2,8-C) ~ 131.5 (12,18- and 13,17- and 2,8- or 3,7-C), 140.5 (1"-C), 149.0 (2″,6″-C), ~153.5 (broad, 4′,6′-pyrimidinic-C), 160.9, 162.2. Assignments are based on H−C and H−H correlated 2D spectra. UV ($CHCl_3$) λ_{max}, log(ϵ_{max}): 417 (4.64), 446 (3.24), 513 (3.22), 548 (2.83), 586 (2.72), 642 (2.58). IR (KBr): 732 m, 792 s, 916 m, 963 m, 1245 m, 1362 m, 1461 s, 1592 s, 2858 m, 2899 m, 2961 s, 2964 ms, 3304 m. MALDI-TOFF-MS (HABA matrix): m/z = 780.40 (100) [M + H^+]. HR-FAB-MS: m/z = 780.4738; calcd for $C_{52}H_{58}N_7$ = 780.4754.

5-(2-Aminopyrimidin-5-yl)-10,20-bis(3,5-di-*tert*-butylphenyl)-zinc-porphinato (Zn-5). Zinc acetate metalation of **5** in a homogeneous chloroform methanol solution occurs almost quantitatively. Column chromatography on silica gel provides an analytical pure sample. Because of self-assembly, spectra are solvent and temperature dependent (see figures). HR-FAB-MS: m/z = 841.3793; calcd for $C_{52}H_{55}N_7Zn$ = 841.3810.

Crystallographic data (excluding structure factors) for Zn-**5**·2$3(C_6H_{12})$ have been deposited with the Cambridge Crystallographic Data Centre as supplementary publication no. CCDC 186026. Copies of the data can be obtained free of charge on application to CCDC, 12 Union Road, Cambridge CB2 1EZ, UK (Fax: (+44)1223−336−033; e-mail: deposit@ccdc.cam.ac.uk).

5,15-Bis(2-phthalimidopyrimidin-5-yl)-10,20-bis(3,5-di-*tert*-butylphenyl)-21*H*,23*H*-porphine (6). Through a suspension of 2-phthalimido-5-(trimethylstannyl)pyrimidine[15c] (406 mg, 1.05 mmol) and dibromoporphyrin **3** (360 mg, 0.42 mmol) in dry toluene (50 mL) was bubbled argon for 4 min, after which 24.3 mg (5 mol %) of tetrakis-(triphenylphosphine)palladium catalyst was added and the mixture degassed with argon for a further minute and then stoppered and heated on an oil bath at 100 °C for 20 h. Silica gel (5 g) was added to the reaction flask, and the solvent was then evaporated under reduced pressure. Column chromatography on silica gel eluted first with dichloromethane and then with 3% methanol in dichloromethane afforded 43.3 mg of the monocoupled product **4** (11% yield), which had R_F = 0.48 (TLC eluted with 3% MeOH in CH_2Cl_2). The main product had R_F = 0.11 (TLC eluted with 3% MeOH in CH_2Cl_2) and was conveniently eluted from the column with 5% MeOH in CH_2Cl_2. It crystallized after evaporation of the solvents, giving 372.7 mg, (77% yield). Recrystallization was convenient from chloroform/*n*-hexane (1:2, v/v). ^{1}H NMR ($CDCl_3$), δ = 9.75 (s, 4H, 4′,6′-pyrymidinic-H), 9.07 (d, ^3J(H,H) = 4.8 Hz, 4H, β-pyrrolic-H), 8.91 (d, ^3J(H,H) = 4.8 Hz, 4H, β-pyrrolic-H), 8.15 (dd, ^3J(H,H) = 5.4 Hz, ^4J(H,H) = 3.0 Hz, 4H, phthalimido-H), 8.12 (d, ^4J(H,H) = 1.8 Hz, 4H, 2″,6″-H), 7.93 (dd, ^3J(H,H) = 5.4 Hz, ^4J(H,H) = 3.0 Hz, 4H, phthalimido-H), 7.86 (t, ^4J(H,H) = 1.8 Hz, 4H, 4"-H), 1.56 (s, 36H, $C(CH_3)_3$), −2.75 (s, 2H, 21,23-H). ^{13}C NMR ($CDCl_3$), δ = 31.7, 35.1, 110.8, 121.6, 123.2, 124.4, 130.2, 131.8, 135.0, 135.1, 140.4, 149.1, 152.8, 161.4, 166.0. UV ($CHCl_3$) λ_{max}, log(ϵ_{max}): 424 (4.64), 452 (3.41), 520 (3.22), 556 (2.99), 593 (2.73), 651 (2.80). IR (KBr) 531 w, 641 w, 670 m, 704 m, 713 s, 782 m, 799 s, 821 w, 861 mw, 861 m, 881 m, 916 m, 973 s, 1082 m, 1097 mw, 1226 mw, 1249 m, 1373 vs, 1423 vs, 1468 m, 1478 mw, 1592 m, 1728 vs, 1751 s, 1792 mw, 2869 mw, 2905 mw, 2963 s, 3316 mw, 3416 (broad) mw. MALDI-TOFF-MS (HABA matrix): m/z = 1133.55 (100) [M + H^+] calcd for $C_{72}H_{64}N_{10}O_4$ = 1132.511.

5,15-Bis(2-aminopyrimidin-5-yl)-10,20-bis(3,5-di-*tert*-butylphenyl)-21*H*,23*H*-porphine (7). To a solution of 245 mg of **6** in 120 mL of dry, freshly distilled dichloromethane was added 5 mL of methylhydrazine, and the reaction mixture was degassed with argon for 3 min, after which it was stirred for 3 h at room temperature. Silica gel (5.5 g) was added to the flask, and the solvent was removed in a vacuum (Caution: at the end of the evaporation a strongly exothermic adsorption on silica gel occurs due to the residual methylhydrazine. External cooling is recommended). Column chromatography on silica gel eluted with dichloromethane containing 4% MeOH afforded a main fraction (R_F = 0.33) after some faster moving impurities. Recrystallization from hot chloroform, followed by dilution with hexane and cooling overnight at −18 °C followed by filtration and drying afforded 168 mg (89% yield) of **7**. ^{1}H NMR ($CDCl_3$), δ = 9.11 (s, 4H, 4′,6′-pyrimidinic-H), 8.98 (d, ^3J(H,H) = 4.8 Hz, 4H, β-pyrrolic-H), 8.93 (d, ^3J(H,H) = 4.8 Hz, 4H, β-pyrrolic-H), 8.09 (d, ^4J(H,H) = 1.8 Hz, 4H, 2″,6″-H), 7.83 (t, ^4J(H,H) = 1.8 Hz, 4H, 4″-H), 5.44 (s, 4H, NH_2), 1.55 (s, 36H, $C(CH_3)_3$), −2.77 (s, 2H, 21,23-H). ^{13}C NMR ($CDCl_3$), δ = 31.8, ($C(CH_3)_3$), 35.2 ($C(CH_3)_3$), 113.0, 114.6, 121.4, 122.3, 126.6, 130.0 (2″,6″-C), 132.2 (broad, β-pyrrolic-C), ~134.0 (broad, β-pyrrolic-C), 140.9, 149.0, 161.0, 162.4. UV ($CHCl_3$) λ_{max}, log(ϵ_{max}): 424 (4.52), 453 (3.76), 521 (3.07), 557 (2.90), 595 (2.60), 678 (2.91). IR (KBr): 636 w, 716 mw, 724 mw, 732 mw, 794 ms, 884 w, 899 w, 916 mw, 973 ms, 1201 w, 1249 m, 1346 mw, 1362 m, 1393 w, 1461 vs, 1530 w, 1548 w, 1593 vs, 2868 m, 2904 m, 2963 s, 3193m, 3300 m, 3389 ms, 3500 m. MALDI-TOFF-MS (HABA matrix): m/z = 873.63 (100) [M + H^+]. HR-FAB-MS: m/z = 873.5103; calcd for $C_{56}H_{61}N_{10}$ = 873.5081.

5,15-Bis(2-aminopyrimidin-5-yl)-10,20-bis(3,5-di-*tert*-butylphenyl)-21*H*,23*H*-zinc-porphinato (Zn-7). Metalation with zinc acetate of the free base **7** as described above provided after the same workup a pure sample which showed solvent, temperature, and concentration dependent spectra. HR-FAB-MS: m/z = 936.4267; calcd for $C_{56}H_{60}N_{10}Zn$ = 936.4294.

Acknowledgment. This work was partially supported by the Deutsche Forschungsgemeinschaft (DFG) through the joint project C3.2 of the Center for Functional Nanostructures involving FZK-INT and the University of Karlsruhe. The authors would like to thank Matthias Fisher (FZK-INT) and Angelika Dreier (MPI) for valuable assistance. Angelika Kernert (University of Karlsruhe) and Raymond Hueber (Université Louis Pasteur, Strasbourg) are thanked for the FAB mass spectra.

Supporting Information Available: Additional spectral data of self-assembled Zn-**5** and Zn-**7**. This material is available free of charge via the Internet at http://pubs.acs.org.

JA029548R